

Myocardial strain estimated from standard cine MRI closely represents strain estimated from dedicated strain-encoded MRI

Andrew Allan, Hao Gao, Christie McComb and Colin Berry

Abstract—A method of non-rigid image registration was developed and evaluated for the purpose of quantifying myocardial displacement and strain from cine MRI using DENSE MRI as the reference standard. The objective of this paper was to study the potential use of cine MRI with image registration, as a means of measuring strain. The local displacement of the left ventricle was modelled by free-form deformations using b-splines. Cardiac MRI images were obtained from four healthy volunteers at 1.5T and analysed by the implementation of image registration algorithms in cine data and with DENSE view in DENSE data. The results indicated there was less than 3% difference between the strain values obtained from cine and DENSE scans averaging across the regions of the left ventricle in healthy subjects (n=4). There lies great potential in the implementation of cine MRI as a means of strain estimation. As such the measurement of strain from standard cine MRI poses an appealing and potentially clinically useful new option for assessing patients with myocardial dysfunction.

I. INTRODUCTION

Cardiac magnetic resonance imaging is the current gold standard method for determining both global and regional myocardial function [8]. At present, measurement of global myocardial function, such as ejection fraction, wall motion and thickening is inadequate to identify the full extent of cardiac dysfunction. This is due to the lack of sensitivity of global measures to changes in regional performance [11][4]. New accurate tools for measurement of regional function are sought after. Strain imaging has been introduced as one of the prominent tools to best define the degree of myocardial dysfunction. Strain is a property of the contractile function of the heart and is a measure of the relative tissue deformation. By evaluating strain it is possible to localise ischemic heart disease and evaluate the viability of the myocardium [11].

Historically strain was first measured non-invasively after its introduction in 1988 by Zerhouni et al. [12] and in 1989 by Axel and Dougherty [2], using tagging cardiac MRI. At present tagging MRI is the most widely validated tool for quantification of multi-dimensional strain, though

more recently there has been much research carried out into the implementation and use of DENSE (displacement encoded with stimulated echoes) MRI as a means of strain quantification. DENSE is a well established method of strain measurement. A number of recent studies have been carried out, from reconstruction of myocardial tissue motion [6] to the quantification of circumferential strain in the common carotid artery [5]. DENSE MRI's recent application has been due to its advantages over tagging MRI, where DENSE can give higher spatial resolution and more direct computation of displacement [9].

In order to quantify strain from medical images it is necessary to use image registration techniques. The process of image registration is defined as determining a transformation between the spatial coordinates in one image to those in another to achieve biological, anatomical or functional correspondence [7]. Non-rigid transformations incorporate all non-linear forms of deformation and include large degrees of freedom. Non-rigid registration is required for cardiac image analysis. This is due to the complex deformations which occur during the cardiac cycle, and in relation to respiratory motion. Image registration encompasses many different approaches such as intensity, geometric and phase based approaches. Each has its own similarity measure, transformation model and optimisation which are collectively known as the image registration algorithms. Most important of these is the transformation model in which many different model methods exist in order to register medical image data, such as finite element and spline based models.

The objective of this study was to develop a new method for quantifying strain from conventional cine MRI scans using image registration and to compare strain values obtained using DENSE MRI as the reference standard.

II. METHODOLOGY

A. Cardiac Image Acquisition

MRI images were obtained in 4 healthy subjects (3 male, 1 female, age range 22-41). MRI images were acquired on a 1.5 Tesla clinical MRI scanner (Siemens AVANTO) in the Golden Jubilee National Hospital, Glasgow. All acquisitions were carried out by a qualified radiographer. The cine and DENSE scans were spatially co-registered as the axial acquisitions were obtained at the same slice position in the heart.

The imaging study had full research ethics committee approval. Standard clinical settings were used for cine (256 x 144 image matrix, TR 51.48ms, TE 1.21ms, 360 x 255 mm FOV, 7 mm slice thickness, 3mm slice gap) and for

Manuscript received March, 2011. This work was supported by the British Heart Foundation and NHS Scotland

A. Allan is with the BHF Glasgow Cardiovascular Research Centre, University of Glasgow, Glasgow, UK, G12 8TA (email: 0602827a@student.gla.ac.uk)

H. Gao is with Centre for excellence in Signal and Image Processing (CeSIP), University of Strathclyde, Glasgow, UK, G1 1XW (email: hao.gao@eee.strath.ac.uk)

C. McComb is with the Department of Clinical Physics, NHS Greater Glasgow and Clyde, Glasgow, UK (email: christie.mccomb@nhs.net)

C. Berry is with BHF Glasgow Cardiovascular Research Centre, University of Glasgow, Glasgow, UK, G12 8TA (email: colin.berry@glasgow.ac.uk, phone: 44(0) 141 211 6311)

DENSE (128 x 80 image matrix, TR 31ms, TE 2ms, 448 x 280 mm FOV, 8 mm slice thickness, 2 mm slice gap) image acquisition. A single mid-cavity slice from the scan of each healthy subject was used for image analysis. Following this the images were cropped to focus on the left ventricle (LV).

B. Non-Rigid Registration

Image analysis of cine MRI images was implemented in Matlab 7.11.0 (R2010b). After importing the cine images into Matlab the image registration algorithms were initiated.

1) *Similarity Measure*: By measuring the intensity error between the two images adjustments are made to the transformation to maximize the similarity between images. In this study the similarity measure used was a correlation based method considering sum of squared differences (SSD) as defined below in equation (1).

$$C_{similarity} = \frac{1}{N} \sum_i (I1(p_i) - I2(T(p_i)))^2 \quad (1)$$

where N is the number of total pixels, I1 is the reference image, I2 image is the current image, p_i is the pixel position in I1 and T is the current transformation estimate such that $T(p_i)$ is the corresponding pixel position in I2.

2) *Transformation Model*: The transformation model used within this study was uniform cubic B-splines. B-splines are computationally efficient and have local support at each knot point. The basic concept behind this method is in manipulating an initial grid mesh of control points overlaying an image, with domain, $\Omega = (x, y) \mid 0 \leq x < X, 0 \leq y < Y$. With Φ representing the 2-D mesh of control points $\phi_{i,j}$ with uniform spacing δ . Letting $T : (x, y) \mapsto (x', y')$ be the transformation of any point (x, y) within the reference image domain to its corresponding point (x', y') in the current image. The non-rigid transformation can be defined as:

$$T(x, y) = \sum_{l=0}^3 \sum_{m=0}^3 B_l(u) B_m(v) \phi_{i+l, j+m} \quad (2)$$

where $i = \lfloor x/\delta \rfloor - 1$, $j = \lfloor y/\delta \rfloor - 1$, $u = x/\delta - \lfloor x/\delta \rfloor$ and $v = y/\delta - \lfloor y/\delta \rfloor$.

A penalty term was used to regularise the B-spline transformation and smooth it out, taking the form:

$$C_{smooth} = \frac{1}{A} \int \int_{\Omega} \left(\frac{\partial^2 T}{\partial x^2} \right)^2 + 2 \left(\frac{\partial^2 T}{\partial x y} \right) + \left(\frac{\partial^2 T}{\partial y^2} \right)^2 dx dy \quad (3)$$

where A denotes the area of the image domain.

3) *Optimisation*: The optimisation used within this study was the limited memory Quasi Newton Broyden-Fletcher-Goldfarb-Shanno (L-BFGS) method. The cost function is made up of the cost associated with the image similarity and the smoothness of the transformation and was defined as:

$$C(\Phi) = -C_{similarity}(I1, T(I2)) + \lambda C_{smooth} \quad (4)$$

where $\lambda = 0.01$ is the weighted parameter.

C. DENSE View

Image analysis of DENSE images was carried out in DENSE view which is a programme that allows displacement maps and strain graphs to be obtained from the DENSE MRI scans. This programme has been validated by different research groups, in rotating phantoms [1] and using tagged MRI as a reference standard for comparison [4].

III. RESULTS

A. Displacement Maps

Image analysis of the cine images gave the corresponding transformations for each image data set, from end-diastole to end-systole to end-diastole, considering each image frame for the whole cardiac cycle. These transformations were then projected onto displacement maps to generate the LV motion and displacement. Cine displacement maps were calculated for each transformation in each volunteer data set and compared in a qualitative manner against the corresponding DENSE displacement maps, where Fig. 1 shows an example of a typical output obtained from cine image analysis.

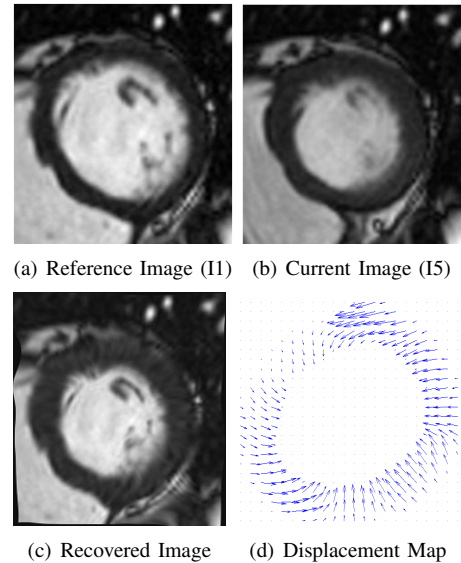


Fig. 1. Standard output

Image (a) refers to the initial input image which is mapped to the current image (b), which represents some deformed version of the initial image. The recovered image (c) shows the image reconstructed from the transformation and the corresponding displacement map (d). Displacement maps

showed good correlation to deformation found in corresponding cine images.

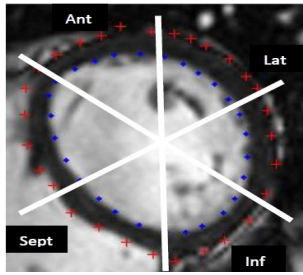


Fig. 2. LV contour drawing of endocardial and epicardial surfaces and segmentation [3]

B. Circumferential Strain

In order to obtain circumferential strain values each initial LV image was segmented into six regions: anterior, lateral, inferior lateral, inferior, inferior septum and anterior septum. An indication of these areas of segmentation can be seen in the LV cine image in Fig. 2, using standardised myocardial segmentation protocols [3].

The arc length for each segment was calculated for the initial LV image then the points in the image domain were displaced using their corresponding displacement from the transformation field. As each point was displaced and tracked the new arc length could be measured to calculate the circumferential strain, where strain was defined as:

$$\text{Circumferential Strain} = \frac{l_1 - l_0}{l_0} \quad (5)$$

where l_0 is the initial arc length and l_1 is the new arc length.

C. Comparison

The comparison between the cine displacement maps and the DENSE displacement maps showed good correlation. However in general the vectors within the cine displacement maps were orientated purely in the radial direction whereas the vectors within the DENSE displacement maps were orientated in both the radial and circumferential direction. An example of a typical cine displacement map and DENSE displacement map is shown in Fig. 3.

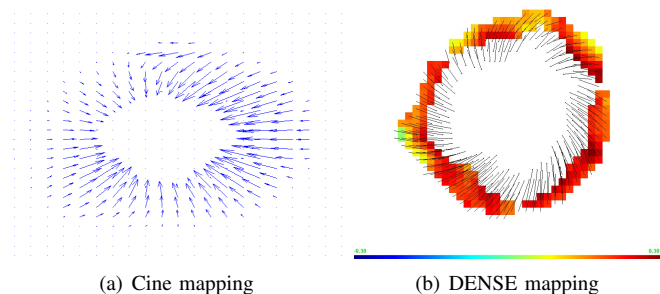
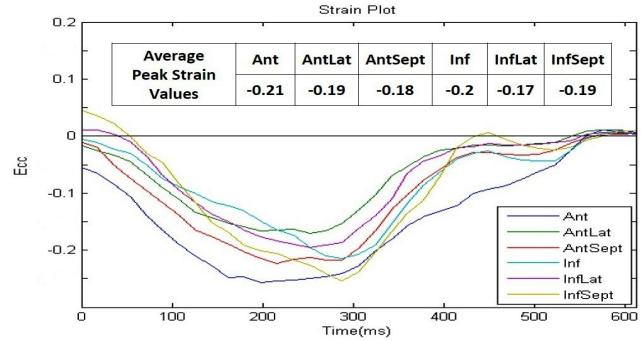
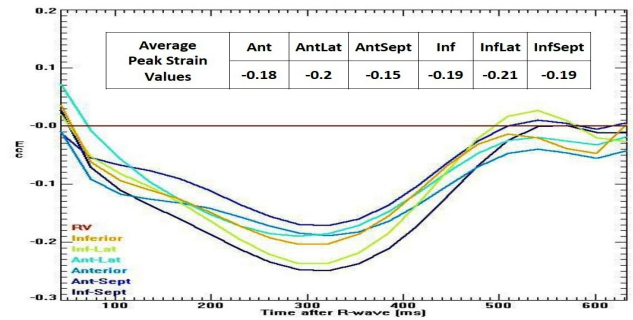


Fig. 3. Displacement maps for cine and DENSE

In particular when comparing the strain curves obtained from both cine and DENSE there was little difference found between the two plots, where the average percentage difference considering peak strain values was less than 3%. An example of a cine and DENSE strain curve obtained can be seen in Fig. 4. The average peak strain values for the healthy subjects ($n=4$) is included as shown.



(a) cine strain plot



(b) DENSE strain plot

Fig. 4. Plot of circumferential strain versus time with separate graph lines for each segment of the left ventricle, including average peak strain values for each LV segment.

D. Statistical Study

Good linear correlation is observed in Fig. 5, which compares circumferential strain measured from cine and DENSE data across the whole cardiac cycle in all 4 healthy subjects. Furthermore the results of Bland-Altman analysis show good agreement is found for strain measurements comparing cine against DENSE, as shown in Fig. 6.

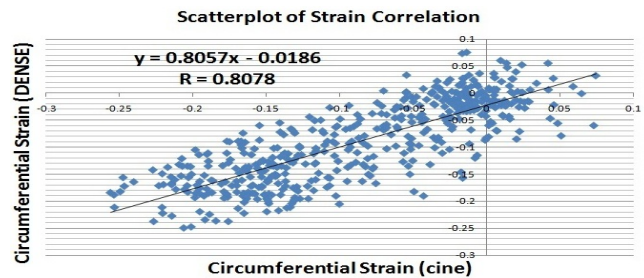


Fig. 5. Scatterplot of circumferential strain values for cine and DENSE methods shows good linear correlation with slope of 0.8057 and $R = 0.8078$.

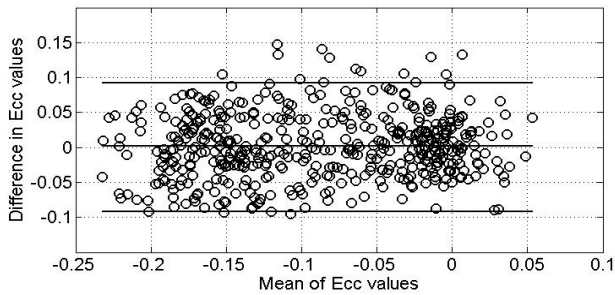


Fig. 6. Bland-Altman plot shows good agreement between circumferential strain values obtained from cine and DENSE methods.

IV. DISCUSSION

This study set out to determine whether or not cine MRI scans could be used to estimate myocardial strain, which is normally calculated from specialised MRI methods. The main finding was that a method which involved non-rigid image registration using b-splines enabled strain estimation from cine as compared to DENSE (a reference method), with a high degree of accuracy in healthy volunteers. After estimating the strain values for cine and comparing to the corresponding DENSE values, analysis of the results showed promising outcomes, with good correlation between the values obtained.

Strain calculations were carried out using an unrefined method for the cine data. DENSE view is a refined and validated method for measuring strain for DENSE data. This can be observed in Fig. 4 where small differences in strain values between cine and DENSE occurred. The small difference in tissue volume imaged, where slice thickness was 7mm in cine and 8mm in DENSE, may have contributed to the differences in strain estimation. Furthermore, temporal differences in strain values were present at certain points in time. This may be due to differences in temporal sensitivity for the two methods of image analysis, where for image acquisition cine MRI (TR 51.48ms) has a higher temporal resolution than DENSE (TR 31ms).

Imaging of the heart is crucial for assessing patients with known or suspected heart disease. The pump function of the heart is particularly important determinant of survival. Since myocardial strain may be a stronger predictor of survival than measurement of left ventricular ejection fraction [10], new methods which enable strain assessment have emerging importance. Strain assessment with echocardiography is limited by problems such as poor acoustic windows. MRI is not limited by this type of problem but instead the MRI methods that are involved for estimating myocardial strain (such as tagging and DENSE), must be acquired, in addition to standard cine imaging for mass and function. The strain MRI methods involve extra breath-holds which contribute to longer scan times overall that may not be well tolerated by unwell patients. Furthermore, tagging and strain-encoded MRI with DENSE involve in-depth image post processing due to lack of automation. Therefore, a new method which could enable strain estimation from standard cine MRI scans

would be appealing and potentially clinically useful. The new method we have developed to estimate strain from cine MRI could represent a new option.

Our future work will focus on the development of a processing method that enables strain to be estimated by imaging clinicians who are not expert in computing. A limitation to the study was the low number of subjects which will be rectified in future studies involving further validation work experimentally and in patients with pathological hearts.

V. CONCLUSIONS

The utilisation of cine MRI for strain measurement by using a non-linear registration method adopted in the study was capable of recovering local strain information from cine MRI. The results indicated there was less than 3% difference between the strain values obtained from cine and DENSE scans averaging across the regions of the left ventricle in healthy subjects (n=4). As such the measurement of strain from standard cine MRI poses an appealing and potentially clinically useful new option for assessing patients with myocardial dysfunction.

REFERENCES

- [1] A. Aletras, R. Balaban, and H. Wen, "High-resolution strain analysis of the human heart with fast-DENSE," *Journal of Magnetic Resonance*, vol. 140, no. 1, pp. 41–57, 1999.
- [2] L. Axel and L. Dougherty, "MR imaging of motion with spatial modulation of magnetization," *Radiology*, vol. 171, no. 3, p. 841, 1989.
- [3] M. Cerqueira, N. Weissman, V. Dilsizian, A. Jacobs, S. Kaul, W. Laskey, D. Pennell, J. Rumberger, T. Ryan, and M. Verani, "Standardized myocardial segmentation and nomenclature for tomographic imaging of the heart: a statement for healthcare professionals from the Cardiac Imaging Committee of the Council on Clinical Cardiology of the American Heart Association," *Circulation*, vol. 105, no. 4, p. 539, 2002.
- [4] D. Kim, W. Gilson, C. Kramer, and F. Epstein, "Myocardial Tissue Tracking with Two-dimensional Cine Displacement-encoded MR Imaging: Development and Initial Evaluation1," *Radiology*, vol. 230, no. 3, p. 862, 2004.
- [5] A. Lin, E. Bennett, L. Wisk, M. Gharib, S. Fraser, and H. Wen, "Circumferential strain in the wall of the common carotid artery: Comparing displacement-encoded and cine MRI in volunteers," *Magnetic Resonance in Medicine*, vol. 60, no. 1, pp. 8–13, 2008.
- [6] Y. Liu, H. Wen, R. Gorman, J. Pilla, J. Gorman III, G. Buckberg, S. Teague, and G. Kassab, "Reconstruction of myocardial tissue motion and strain fields from displacement-encoded MR imaging," *American Journal of Physiology-Heart and Circulatory Physiology*, vol. 297, no. 3, p. H1151, 2009.
- [7] D. Rueckert, L. Sonoda, C. Hayes, D. Hill, M. Leach, and D. Hawkes, "Nonrigid registration using free-form deformations: application to breast MR images," *Medical Imaging, IEEE Transactions on*, vol. 18, no. 8, pp. 712–721, 2002.
- [8] M. Shehata, S. Cheng, N. Osman, D. Bluemke, and J. Lima, "Myocardial tissue tagging with cardiovascular magnetic resonance," *Journal of Cardiovascular Magnetic Resonance*, vol. 11, no. 1, p. 55, 2009.
- [9] B. Spottiswoode, X. Zhong, C. Lorenz, B. Mayosi, E. Meintjes, and F. Epstein, "Motion-guided segmentation for cine DENSE MRI," *Medical image analysis*, vol. 13, no. 1, pp. 105–115, 2009.
- [10] T. Stanton, C. Ingul, J. Hare, R. Leano, and T. Marwick, "Association of myocardial deformation with mortality independent of myocardial ischemia and left ventricular hypertrophy," *JACC Cardiovascular Imaging*, vol. 2, no. 7, p. 793, 2009.
- [11] A. Veress, G. Gullberg, and J. Weiss, "Measurement of strain in the left ventricle during diastole with cine-MRI and deformable image registration," *Journal of biomechanical engineering*, vol. 127, p. 1195, 2005.
- [12] E. Zerhouni, D. Parish, W. Rogers, A. Yang, and E. Shapiro, "Human heart: tagging with MR imaging—a method for noninvasive assessment of myocardial motion," *Radiology*, vol. 169, no. 1, p. 59, 1988.